World Academy of Science, Engineering and Technology
International Journal of Mechanical and Mechatronics Engineering
Vol:18, No:9, 2024

Locomotion Effects of Redundant Degrees of Freedom in Multi-Legged Quadruped Robots

Hossein Keshavarz, Alejandro Ramirez-Serrano

Abstract—Energy efficiency and locomotion speed are two key parameters for legged robots, thus finding ways to improve them are important. This paper proposes a locomotion framework to analyze the energy usage and speed of quadruped robots via a Genetic Algorithm (GA) optimization process. For this, a quadruped robot platform with joint redundancy in its hind legs that we believe will help multi-legged robots improve their speed and energy consumption is used. ContinuO, the quadruped robot of interest, has 14 active degrees of freedom (DoFs), including three DoFs for each front leg, and unlike previously developed quadruped robots, four DoFs for each hind leg. ContinuO aims to realize a cost-effective quadruped robot for real-world scenarios with high-speeds and the ability to overcome large obstructions. The proposed framework is used to locomote the robot and analyze its energy consumed at diverse stride lengths and locomotion speeds. The analysis is performed by comparing the obtained results in two modes, with and without the joint redundancy on the robot's hind legs.

Keywords—Genetic algorithm optimization, locomotion path planning, quadruped robots, redundant legs.

I. Introduction

LEGGED machines have the potential to traverse a greater number of terrains when compared to wheeled robots which cannot traverse many of such environments including mountainous terrains, rocky surfaces, and terrains having sharp depression and elevation changes. Among the diverse types of legged robots including humanoids and hexapods, quadruped robots are advantageous from the aspects of stability, control, and manufacturing cost [1]. Current quadruped robots such as BigDog [2], HyQ [3], Cheetah [4], and many others feature low payload-to-weight ratio, and relative low maneuverability limiting their application to somewhat simple tasks such as inspection in simple environments. If quadruped robots are to be deployed to perform advanced tasks in complex environments (e.g., urban search and rescue within collapsed buildings) their speed, locomotion, and other capabilities must be enhanced [5]. Additionally, energy efficiency and enhanced whole-body mobility are other key parameters that are crucial for enhancing quadruped robots' locomotion. Thus, looking for methods to improve such characteristics is essential. An important and basic component of the design of each quadruped robot, the design of their legs, determines the core application performance of such robots, including their operational adaptability, walking speed, and load capacity [6]. Therefore, the performance improvement of a quadruped robot depends largely on the performance of its mechanical legs.

In nature, animals use a myriad of leg designs (e.g., Digitigrade, Plantigrade, and Unguligrade) which enable felines, bears, and horses, as an example, have diverse strides and leverage. However, the energy usage of such leg designs have not been addressed in the robotics community. Thus, it is important to carry out a comprehensive analysis of the effects of different leg designs with and without redundant joints and linkages. Of special interest is the use and effectiveness of three types of leg designs: prismatic, articulated, and redundant. For a number of years, researchers have developed a variety of quadruped robots with different leg designs to have fast locomotion speeds. The Cheetah and WildCat, robots developed by Boston Dynamics with 3 joints per leg, are the fastest quadruped robots today with galloping capabilities. The Cheetah robot has been registered to achieve a top speed over 12 m/s on a treadmill [7], while the WildCat quadruped robot can reach a top speed of over 8 m/s while maneuvering and maintaining its balance [8].

Quadruped robots with redundant legs are another class of robots designed, at least in theory, to increase speed by adding one or more joints to the traditional 3 DoFs used in quadruped robots. Garcia et al. developed a redundant articulated hybrid mechanical leg (HADE) simulating the horse leg structure [9] having good leg mass distribution, good elastic energy recovery, and high speed. Kim et al. designed a redundant articulated leg based on the leg structure of cheetahs that provides a unique combination of high torque density, high-bandwidth force control, and the ability to mitigate impacts through backdrivability [10]. Inspired by cats, Ijspeert et al. developed the Cheetah-cub series of quadruped robots with redundant articulated legs [11]. Boston Dynamics developed the BigDog quadruped robot with redundant articulated legs (the world's most advanced robot for adapting to rugged terrain) [2]. Redundant articulated legs have been bio-inspired from toed and hoofed animals such as dogs, felines, and deer. This paper concentrates on the study of additional degrees of freedom (DoFs) to the architecture of legs seen in typical quadruped robots (having 3 DoFs per leg) and analyzing how such additional characteristics affect locomotion speed and cost of transport (CoT). For this, a newly developed quadruped robot inspired by Cheetahs in the animal kingdom named *ContinuO* having one additional DoFs in its hind legs is used (Fig. 2).

ContinuO has 14 active DoFs, including three DoFs for each frontal legs and, unlike previously developed quadruped robots, four DoFs for each hind leg. The redundancy added by the additional DoF adds one linkage to each hind leg as illustrated in Fig. 2. It is believed that such a configuration would provide better kinematic (agility) and locomotion properties. ContinuO aims to realize a cost-effective and

Hossein Keshavarz is with University of Calgary, Canada (e-mail: hossein.keshavarz@ucalgary.ca).

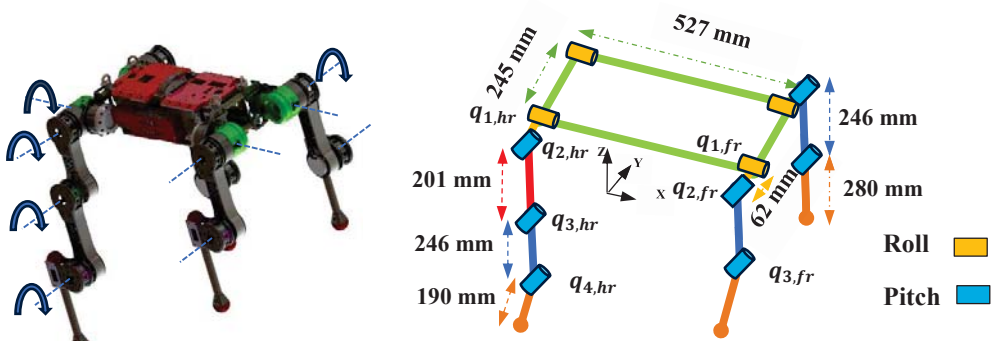

Fig. 1 ContinuO robot and its kinematic characteristics

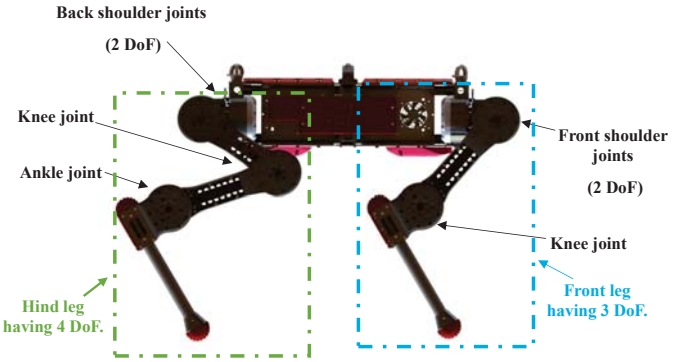

Fig. 2 The ContinuO quadruped robot

TABLE I
CONTINUO ROBOT'S JOINTS (RIGHT SIDE)

Leg	Joint name	Joint	Motion range °
Front	Front shoulder roll	$q_{1,fr}$	[-45°, +45°]
	Front shoulder pitch	$q_{2,fr}$	[-180°, +180°]
	Front Knee	$q_{3,fr}$	[-180°, +180°]
Hind	Back shoulder roll	$q_{1,hr}$	[-45°, +45°]
	Back shoulder pitch	$q_{2,hr}$	[-180°, +180°]
	Back Knee	$q_{3,hr}$	[-180°, +180°]
	Ankle	$q_{4,hr}$	[-180°, +180°]

TABLE II
CONTINUO ROBOT'S MASS DISTRIBUTION

Robot component	Component name	Mass (Kg)
Front Legs	Front hip	1.3
	Front thigh	1.4
	Front shank	0.78
Hind Legs	Back hip	1.3
	Back middle thigh	1.3
	Back thigh	1.4
	Back shank	0.76
Trunk	Body	10.3

anthropomorphic quadruped robot having high-speed, low CoT, and abilities superior to current quadruped robots suitable for real-world scenarios (e.g., search for victims inside collapsed structures). This paper presents a comprehensive analysis on the effects of the additional linkage on the locomotion speed and energy consumption of quadruped robots.

This paper is structured as follows: Section II presents the kinematic structure design of the ContinuO robot. Section III describes the path planning of the robot followed by the robot's inverse kinematic formulations in Section IV. In Section V, the two models used in analyzing the effects of the additional linkage on the performance of two similar size robots are formulated. Finally, Section VI presents simulation results followed by the conclusions in Section VII.

II. MECHANICAL DESIGN

The ContinuO robot has been developed to have a cost-effective quadruped robot for real-world scenarios. The main design concepts of ContinuO include:

- Additional DoFs in the hind legs for increased speed.
- Minimizing overall mass for lower CoT.
- Anthropomorphic design via bioengineering for increased speed.

Most of conventional quadruped robots like BigDog, HyQ and many others have three rotational DoFs in each leg including one-DoF in the hip (in the roll direction), one-DoF in the shoulder (in the pitch direction) and one-DoF in the knee (in the pitch direction). In the ContinuO robot, however, the hind legs have four DoFs and this redundancy aims to help the robot to locomote with higher speeds and lower energy consumption. These leg joints with their rotational axis are shown in Fig. 1. Tables I and II provide summaries of the ContinuO robot's right side joints range of motion and mass distribution of the robot. The range of motion for the left side joints, $q_{i,fl}$ and $q_{j,hl}$, also follow Table I, where i, fl and j, hl denote joint i $(i = 1,2,3)$ for the front left and joint j $(j = 1,2,3,4)$ for the hind left leg, respectively.

III. MOTION PLANNING ALGORITHM

To plan the robot's movements of its legs and body, a path planning locomotion framework based on a Genetic

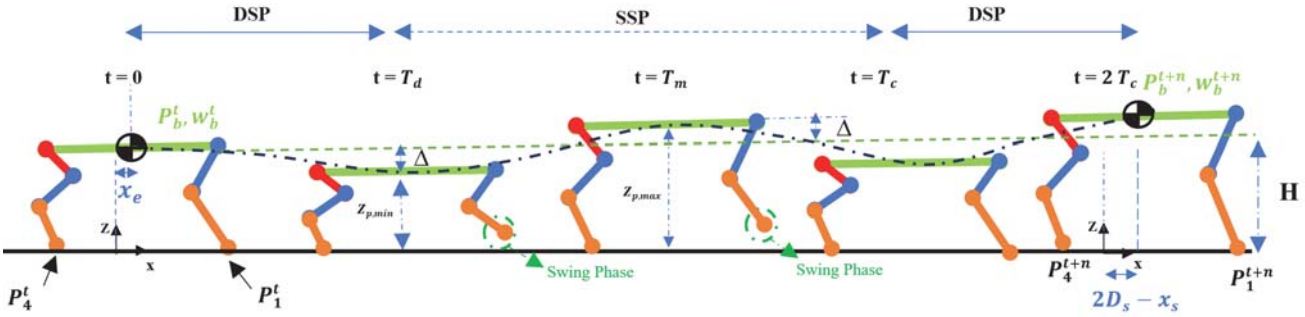

Fig. 3 Visual representation of path planning parameters in the sagittal plane

Algorithm (GA) optimization process is used. In the GA optimization process, the feet and robot's body paths are generated based on a set of optimization variables which uses a set of constraints such as joint limits and the position of the robot's Center of Mass (CoM) over the complete locomotion cycle as illustrated in Fig. 3. Similar to [12], the method of planning a walking pattern consists of the feet and robot's body trajectories. This path generation routine is based on the position ($P_i^t = [x_i^t, y_i^t, z_i^t]$, i= 1 to 4) of each foot at time t and the body position ($P_b^t = [x_b^t, y_b^t, z_b^t]$) and its orientation ($w_b{}^t = [\phi^t, \theta^t, \psi^t]$= $[roll^t, pitch^t, yaw^t]$) in the task space at time t. For the purpose of this paper, any changes in the robot's body orientation are not considered and the robot's orientation remains horizontal and parallel to the horizon during the entire locomotion cycle. Thus, the robot is constrained to maintain a body orientation having zero degrees in its roll, pitch and yaw orientations. As a result, the robot is constrained to be always parallel to the ground on which it is walking, galloping, etc. The trajectory of the body is generated using the set of constraints described by (1) and (2), where the position of the body in the x and z directions is constrained to follow the feet positions accordingly while the body's height is allowed to deviate from a desired height, H, by $\pm\triangle$ as illustrated in Fig. 3.

$$x_b = \begin{cases} x_e & t = 0 \\ D_s - x_s & t = T_d \\ D_s + x_e & t = T_c \\ 2D_s - x_s & t = T_c + T_d \end{cases} \quad (1)$$

$$z_b = \begin{cases} z_{p-min} & t = \frac{T_d}{2} \\ z_{p-max} & t = T_d + \frac{T_s}{2} \\ z_{p-min} & t = T_c + \frac{T_d}{2} \\ z_{p-max} & t = T_c + T_d + \frac{T_s}{2} \end{cases} \quad (2)$$

The terms in (1) and (2) are described in Table III. The constrains for generating the path of each foot rely on the position of the corresponding leg at time t. As an example, the constraints for the front right leg (Leg 1), in the x and z directions are represented by (3) and (4).

$$x_1 = \begin{cases} 0.5l_b & t = 0 \\ 0.5l_b & t = T_d \\ 0.5l_b + D_s & t = T_m \\ 0.5l_b + 2D_s & t = T_c \end{cases} \quad (3)$$

$$z_1 = \begin{cases} 0 & t = 0 \\ 0 & t = T_d \\ h_{max} & t = T_m \\ 0 & t = T_c \end{cases} \quad (4)$$

where, the parameters used in the above equations are defined in Table III.

TABLE III
DESCRIPTION OF THE GAIT PARAMETERS

Parameters	Description
D_s	Stride length
T_c	Walking cycle time
T_d	Time in Double Support (DS)
T_s	Time in Single Support (SS)
T_m	Half of the Single support (SS) time
DSP	Double support phase
SSP	Single support phase
x_e	Distance traveled of the body at T_m
x_s	Distance traveled of the body and stance ankle at the end of SS
Δ	Maximum body motion deviations in the z direction
h_{max}	Maximum height of the foot in a swing phase
l_b	Body length of the robot

Fig. 3 provides a visual representation of the above mentioned constraints in which the front right leg is in the swing phase. By using the mentioned constraints, the desired trajectories of each foot and body of the robot are generated. The flowchart of the proposed GA optimization procedure is depicted in Fig. 5.

IV. Inverse Kinematic Formulation

After generating the desired trajectories of the robot's feet and body via the GA motion planning, the joint angles and their derivatives can be computed via inverse kinematics (IK). Solving the IK for the front legs (having 3 DoFs), is somewhat trivial, however, solving it for the hind redundant legs in a close form solution is challenging. In [13], researchers calculated joint angles of robots having redundant DoF by integrating velocities over time without solving IK directly. However, as expected their numerical integration process has errors that need to be resolved. Thus, the method proposed in [14] is used. The solution is divided into two processes.

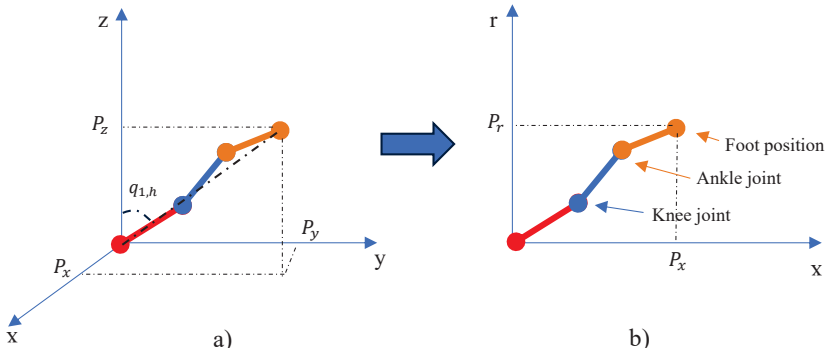

Fig. 4 The new coordinate system for hind legs of the robot

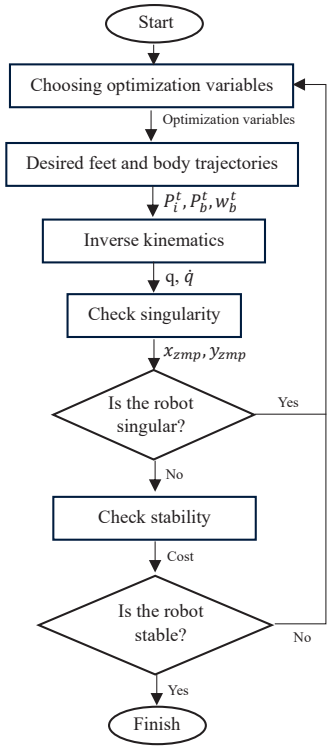

Fig. 5 The flowchart of GA optimization process

The first process computes the hip joint angle (or $q_{1,h}$ in Fig. 4 (a)).

$$q_{1,h} = \arctan(\frac{p_y}{p_z}) \tag{5}$$

where p_y and p_z are the relative positions of the corresponding hind foot with respect to the position of the hip in the y-z plane as shown in Fig. 4b. The second process involves calculating the angles for the remaining joints ($q_{2,h}$, $q_{3,h}$, and $q_{4,h}$). For calculating these angles, a new axis is defined by transferring the Cartesian coordinate system to a polar coordinate system as illustrated in Fig. 4 (b) and computed via (6).

$$\begin{aligned} {p_r}^2 &= {p_y}^2 + {p_z}^2, \\ p_r &= \sqrt{{p_y}^2 + {p_z}^2} \end{aligned} \tag{6}$$

To solve the IK problem, there is a need to define a new variable, ε, defined as the summation of joint angles $q_{2,h}$, $q_{3,h}$ and $q_{4,h}$ as defined by (7) and shown in Fig. 6. Solving the IK, at each iteration requires this variable to be known (defining a constraint imposed on the system/leg).

$$\varepsilon = q_{2,h} + q_{3,h} + q_{4,h} \tag{7}$$

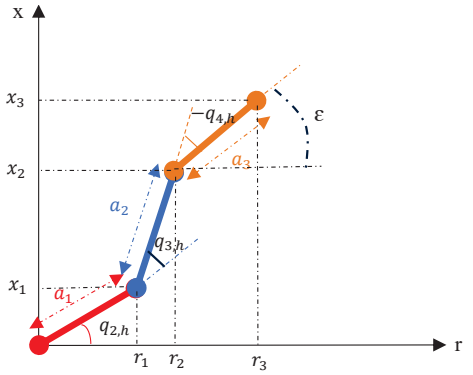

Fig. 6 The inverse kinematic model for hind legs of the robot

The constraint (7) and the angle ε helps to find the orientation of the last link of the leg with respect to the r axis (see Fig. 6). Subsequently, the corresponding ankle position, r_2 and x_2, can be calculated using (8):

$$\begin{aligned} r_2 &= r_3 - a_3 cos(\varepsilon) \\ x_2 &= x_3 - a_3 sin(\varepsilon) \end{aligned} \tag{8}$$

where, r_3 and x_3 are the desired foot position (see Fig. 6) calculated using the path planning method (Section III). Hence, via the geometry of the leg, the joint angle, $q_{3,h}$, is calculated by using the sine rule as follows:

$$q_{3,h} = \pm \arccos \frac{{r_2}^2 + {x_2}^2 - ({a_1}^2 + {a_2}^2)}{2a_1a_2} \tag{9}$$

After calculating $q_{3,h}$ and having ε, one can calculate the joint angle $q_{2,h}$ as follows (11):

$$\begin{aligned} r_2 &= a_1 cosq_{2,h} + a_2 cos(q_{2,h} + q_{3,h}) \\ z_2 &= a_1 sinq_{2,h} + a_2 sin(q_{2,h} + q_{3,h}) \end{aligned} \tag{10}$$

$$q_{2,h} = \arctan(\frac{sinq_{2,h}}{cosq_{2,h}}) \tag{11}$$

Finally, by using (7), (12) can be obtained to find $q_{4,h}$.

$$q_{4,h} = \varepsilon - q_{2,h} - q_{3,h} \tag{12}$$

After calculating the joint positions, velocities and accelerations, the ZMP criterion is used to evaluate the stability of the robot which defines a cost function for the optimization process [15].

V. Models

To analyze the speed and energy consumption of the robot, two models of the robot are considered enabling us to compare similar size robots having different kinematic and locomotion characteristics: i) robot model having redundancy in the hind legs, and ii) robot having 3 DoFs per leg like most available quadruped robots. Fig. 7 illustrates the two models schematically.

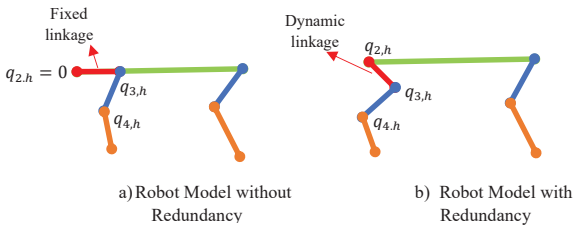

Fig. 7 The two models of the ContinuO robot used

For generating the model without redundancy (Fig. 7a), the additional back shoulder joint, $q_{2,h}$ (see Fig. 2) is fixed to zero degrees (parallel to the robot's body). However, in the model with redundancy such joint is not constrained and as a result participates in the robot's locomotion.

VI. Results

In this section, the simulation results for energy usage and speed of the quadruped robot ContinuO on the two hind leg models are presented. The results are discussed based on the following three aspects:

- Singularity of the joints
- Energy consumption of the robot
- The power consumption by the joints

A. Singularity of the Joints

Joint singularities in legged robots can occur in various situations, depending on the robot's design, configuration, and the specific task it is performing. Herein, joint singularities are defined as joint angles that result in the two leg links interconnected by the joint are collinear. Joint singularities can result from the computation of inverse kinematics, where the robot calculates the joint angles required to achieve a specific end-effector position or trajectory. In some cases, there may be multiple solutions or discontinuities in the inverse kinematics, leading to singular configurations. To achieve high speeds in legged locomotion, the robot typically needs to use larger stride lengths. Hence, the two hind leg models (Fig. 7) are compared for different stride lengths.

The most important joint in terms of singularity is the knee joint. Thus, to check for singularity, large stride lengths are considered and the two robot models are compared when the robot is trotting with a speed of 0.1 $\frac{m}{s}$ and a stride length is 0.20 m which is considered a large stride for the robot. Figs. 8 and 9 show that in large stride lengths, the model having redundancy (Fig. 7 (b)) in the hind legs does not reach a singularity position (Fig. 8) while in the other model, the knee joint reaches singular positions in the hind legs (Fig. 9). Furthermore, the results show that when increasing the stride length the speed of the robot increases proportionally to the increase in the stride. However, the robot tends to reach a singularity point more often.

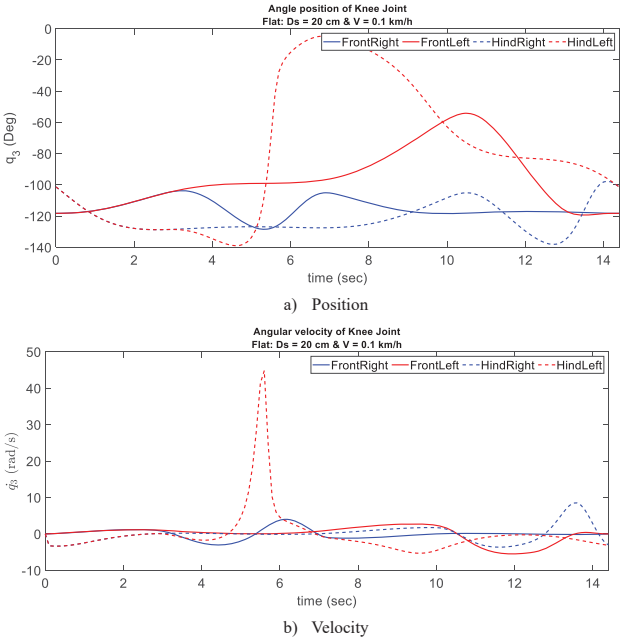

Fig. 8 Motion of knee joints for the leg with redundancy

B. Energy Consumption of the Robot

Another important parameter is the energy consumption of the robot in different conditions. To evaluate the two robot models, four speeds and stride lengths were analyzed. Before such analysis the path for the feet and the robot's COM was optimized for each of the selected speed and stride lengths. Finally, the total power consumption for each model under the same speed was compared. Figs. 10 and 11 provide the obtained results in the form of a 3D surface representing the consumed power by the robot as a function of the stride length and the speed. From such figures, it can be seen that in the robot without redundancy (Fig. 10) the consumed power is uniform but it shows a sharp power increase when the robot reaches a specific stride length threshold. This can be clearly seen when large stride lengths are used (larger than 0.2 m). Such increase in CoT might also be attributed to the fact that the leg experiences joint singularities. In contrast, the model with redundancy (Fig. 11) provides a gradual increase throughout the speed and stride length as joint singularities are

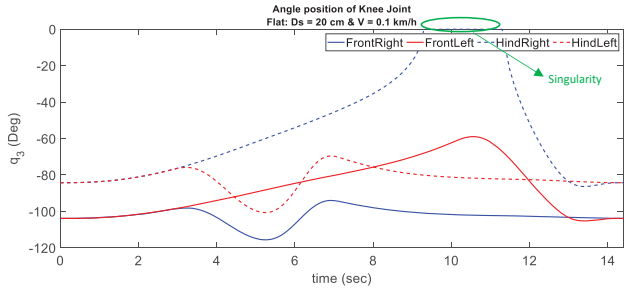

a) Position

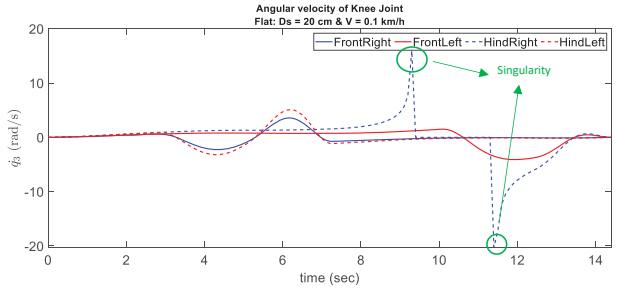

b) Velocity

Fig. 9 Motion of knee joints for the leg without redundancy

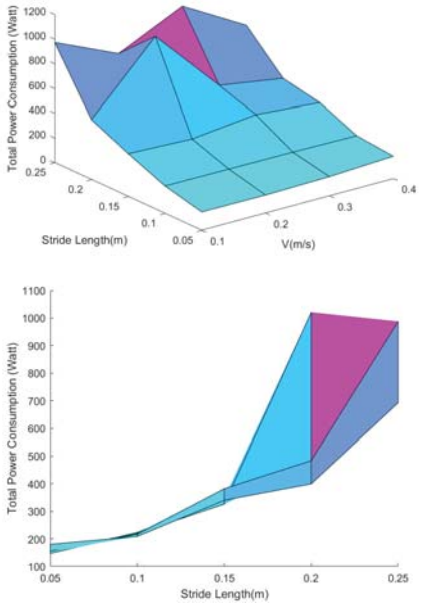

Fig. 10 Total power consumption with respect to speed and stride length for the non-redundant model

not observed. The results provided by the leg with redundancy can be used to better manage speed vs the power consumed by the robots which provide important information to perform smoother locomotion transitions while better managing power resources.

C. Power Consumption by the Robot's Joints

In addition to the total power consumption, the power consumption by each of the robot's joints was also analyzed.

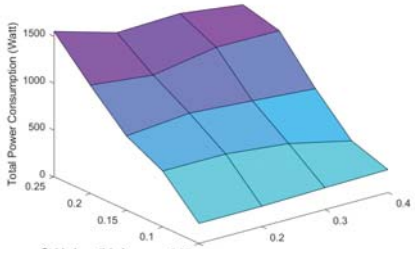

Fig. 11 Total power consumption with respect to speed and stride length for the model with redundancy

Here, the power consumption of the knee joints of the Front Right (FR) and the Hind Right (HR) legs of the robot were compared under different speeds and stride lengths.

The results of such work are provided in Tables IV-VI. Table IV provides the results at low speeds and short stride lengths (V = 0.1 $\frac{m}{s}$ and D_s = 0.05 m).

TABLE IV
POWER CONSUMPTION AT LOW SPEED AND SHORT STRIDE LENGTH

Models	Knee joint (FR leg)	Knee joint (HR leg)
Redundant Model	21.1133 (W)	10.9667 (W)
Non-redundant Model	15.2603 (W)	19.9452 (W)

Based on the results in Table IV, the non-redundant leg has better power consumption on the frontal knee but lower power on the hind leg. The opposite is seen in the redundant model.

Table V shows the results at mid speeds and high stride lengths (V = 0.2 $\frac{m}{s}$ and D_s = 0.2 m):

TABLE V
POWER CONSUMPTION AT MID SPEED AND HIGH STRIDE LENGTH

Models	Knee joint (FR leg)	Knee joint (HR leg)
Redundant Model	59.8641 (W)	25.6877 (W)
Non-redundant Model	70.8932 (W)	140.6294 (W)

By increasing the locomotion speed and stride length, the redundant model has better power consumption for both hind and front legs. Specially for the hind legs, the benefits of redundancy on the knee joint in terms of energy consumed is enormous.

Finally, Table VI shows the results for the robot locomotion at high speeds and high stride lengths (V = 0.3 $\frac{m}{s}$ and D_s = 0.2 m).

TABLE VI
POWER CONSUMPTION AT HIGH SPEED AND STRIDE LENGTH

Models	Knee joint (FR leg)	Knee joint (HR leg)
Redundant Model	68.6561 (W)	28.4635 (W)
Non-redundant Model	37.8383 (W)	63.3569 (W)

The results in Table VI are similar to when the robot moves at low speeds with short stride lengths (Table IV).

VII. Conclusions

The obtained results show that robot legs with redundant joints/linkages help the robot to have large stride lengths without singularity in the knee joints considered the most important joint during locomotion. Also, the energy consumption seen in redundant legs has a uniform behavior with increasing stride length and speed. But in the non-redundant model, energy consumption has a nonuniform and nonlinear behaviour. Thus, by increasing the stride length, the rate of change of the energy consumption in different velocities is different. In addition, by increasing the speed and the stride length of the robot, the energy consumption of the knee joints is lower when compared to legs having no redundancy. Also, in the redundant model, the power consumption of the hind legs knee joint is lower than the similar joint in the front legs. Such observations indicate that when we have redundancy, the power consumption will decrease in the joint space.

Finally, the effects of additional linkages on the speed and energy consumption of the robot provide benefits that can be exploited reducing power consumption while increasing locomotion speed.

References

[1] J. Wang, K. Lu, S. Xu, and Y. Lei, "Research situation and prospect on quadruped walking robot," *Manuf Autom*, vol. 31, no. 2, pp. 4–6, 2009.

[2] M. Raibert, K. Blankespoor, G. Nelson, and R. Playter, "Bigdog, the rough-terrain quadruped robot," *IFAC Proceedings Volumes*, vol. 41, no. 2, pp. 10 822–10 825, 2008.

[3] C. Semini, N. G. Tsagarakis, E. Guglielmino, M. Focchi, F. Cannella, and D. G. Caldwell, "Design of hyq–a hydraulically and electrically actuated quadruped robot," *Proceedings of the Institution of Mechanical Engineers, Part I: Journal of Systems and Control Engineering*, vol. 225, no. 6, pp. 831–849, 2011.

[4] S. Seok, A. Wang, M. Y. Chuah, D. Otten, J. Lang, and S. Kim, "Design principles for highly efficient quadrupeds and implementation on the mit cheetah robot," in *2013 IEEE International Conference on Robotics and Automation*. IEEE, 2013, pp. 3307–3312.

[5] Y. Wang and S. Boyd, "Fast model predictive control using online optimization," *IEEE Transactions on control systems technology*, vol. 18, no. 2, pp. 267–278, 2009.

[6] S. Seok, A. Wang, M. Y. Chuah, D. J. Hyun, J. Lee, D. M. Otten, J. H. Lang, and S. Kim, "Design principles for energy-efficient legged locomotion and implementation on the mit cheetah robot," *Ieee/asme transactions on mechatronics*, vol. 20, no. 3, pp. 1117–1129, 2014.

[7] B. Dynamics, "Cheetah robot runs 28.3 mph; a bit faster than usain bolt," 2009.

[8] Introducing wildcat. [Online]. Available: https://www.youtube.com/watch?v=wE3fmFTtP9g

[9] E. Garcia, J. C. Arevalo, G. Muñoz, and P. Gonzalez-de Santos, "Combining series elastic actuation and magneto-rheological damping for the control of agile locomotion," *Robotics and Autonomous Systems*, vol. 59, no. 10, pp. 827–839, 2011.

[10] H.-W. Park and S. Kim, "The mit cheetah, an electrically-powered quadrupedal robot for high-speed running," , vol. 32, no. 4, pp. 323–328, 2014.

[11] A. Spröwitz, A. Tuleu, M. Vespignani, M. Ajallooeian, E. Badri, and A. J. Ijspeert, "Towards dynamic trot gait locomotion: Design, control, and experiments with cheetah-cub, a compliant quadruped robot," *The International Journal of Robotics Research*, vol. 32, no. 8, pp. 932–950, 2013.

[12] M. Sadedel, A. Yousefi-Koma, M. Khadiv, and M. Mahdavian, "Adding low-cost passive toe joints to the feet structure of surena iii humanoid robot," *Robotica*, vol. 35, no. 11, pp. 2099–2121, 2017.

[13] G. Lu, T. Chen, Q. Liu, G. Zhang, X. Rong, and S. Wang, "A novel multi-configuration quadruped robot with redundant dofs and its application scenario analysis," in *2021 International Conference on Computer, Control and Robotics (ICCCR)*. IEEE, 2021, pp. 14–20.

[14] H. Z. Ting, M. Hairi, M. Zaman, M. Ibrahim, and A. Moubark, "Kinematic analysis for trajectory planning of open-source 4-dof robot arm," *International Journal of Advanced Computer Science and Applications*, vol. 12, no. 6, pp. 769–777, 2021.

[15] Q. Huang and Y. Nakamura, "Sensory reflex control for humanoid walking," *IEEE Transactions on Robotics*, vol. 21, no. 5, pp. 977–984, 2005.

Hossein Keshavarz H. Keshavarz received his M.Sc. degree in Mechanical engineering from the University of Tehran, Tehran, Iran. He is currently Ph.D. student in mechanical engineering at the University of Calgary under the supervision of Dr. Alejandro Ramirez-Serrano. His research interests include robust motion planning, and optimal control of agile robotic systems.

Alejandro Ramirez-Serrano Alex Ramirez-Serrano (Member, IEEE) received the B.Sc. degree in mechanical engineering from Mexico, the dual M.Sc. degrees in mechanical and aerospace engineering and computer science/artificial intelligence from USA and Mexico, respectively, and the Ph.D. degree in mechanical and industrial engineering from Canada. He is currently a full time Professor with the University of Calgary, where he has served on diverse roles, including the Former Director of the Manufacturing Program and the Director of the Graduate Program with the Department of Mechanical and Manufacturing Engineering. He is also the Founder and the Director of the Unmanned Vehicle Systems (UVS) Robotarium Research Laboratory, where he performs research and development activities in-ground, aerial, and humanoid robotics. He is also the Founder and the Chief Executive Officer (CEO) at 4Front Robotics, a Canadian-based robotics company developing UVS for operation in confined complex spaces. His research interest includes the design, control, navigation, and modeling of UVS.